Nanoplatforms for Targeted Molecular Imaging in Living Subjects

Weibo Cai and Xiaoyuan Chen*
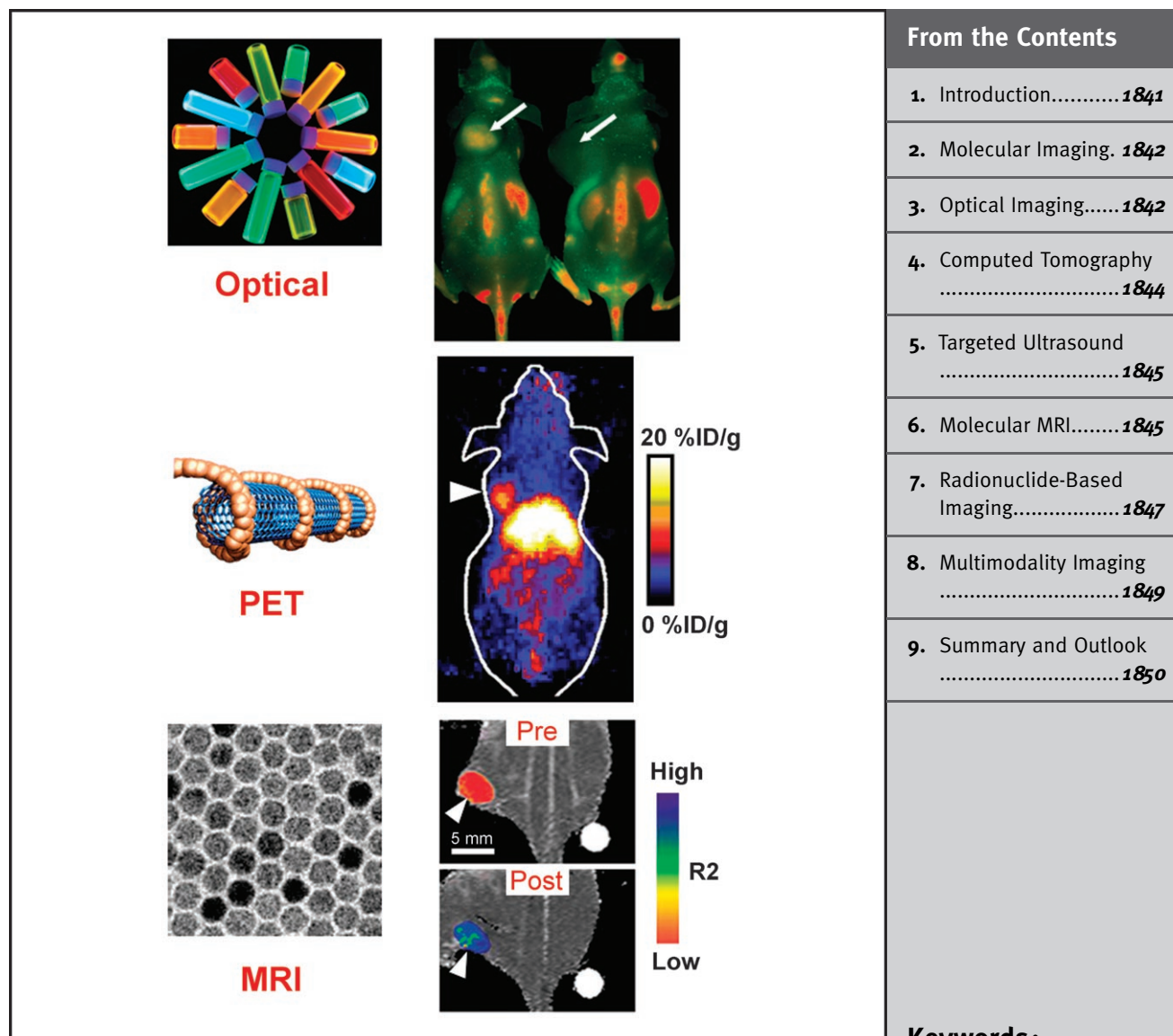
Optical

20 %ID/g

0 %ID/g

PET

Pre

High

5 mm

R2

Post

Low

MRI

Various methods have been employed to image the interior of living entities.

From the Contents

Keywords:
- cancer
- molecular imaging
- nanomedicine
- nanoplatforms
- nanotechnology

small
NANO MICRO

*M*olecular or personalized medicine is the future of patient management and molecular imaging plays a key role towards this goal. Recently, nanoplatform-based molecular imaging has emerged as an interdisciplinary field, which involves chemistry, engineering, biology, and medicine. Possessing unprecedented potential for early detection, accurate diagnosis, and personalized treatment of diseases, nanoplatforms have been employed in every single biomedical imaging modality, namely, optical imaging, computed tomography, ultrasound, magnetic resonance imaging, single-photon-emission computed tomography, and positron emission tomography. Multifunctionality is the key advantage of nanoplatforms over traditional approaches. Targeting ligands, imaging labels, therapeutic drugs, and many other agents can all be integrated into the nanoplatform to allow for targeted molecular imaging and molecular therapy by encompassing many biological and biophysical barriers. In this Review, we will summarize the current state-of-the-art of nanoplatforms for targeted molecular imaging in living subjects.

1. Introduction

Nanotechnology, an interdisciplinary research field involving chemistry, engineering, biology, medicine, and more, has great potential for early detection, accurate diagnosis, and personalized treatment of diseases. Nanoscale devices are typically smaller than several hundred nanometers and are comparable to the size of large biological molecules such as enzymes, receptors, and antibodies. With a size about 100 to 10000 times smaller than human cells, these nanoscale devices can offer unprecedented interactions with

biomolecules both on the surface of and inside cells, which may revolutionize disease diagnosis and treatment. The most well-studied nanomaterials include quantum dots (QDs),[1,2] carbon nanotubes,[3,4] nanoshells,[5] paramagnetic nanoparticles,[6] and many others (Figure 1).[7,8]

Over the last decade, there have been numerous nanotechnology centers established worldwide.[9,10] In the United States alone, more than $6 bn has been invested in nanotechnology research and more than sixty centers, networks, and facilities, funded by various agencies, are in operation or soon to open.[11] After establishing an interdisciplinary nanotechnology workforce, it is expected that nanotechnology will mature into a clinically useful field in the near future.

One of the major applications of nanotechnology is in biomedicine. Nanoparticles can be engineered as nanoplatforms for effective and targeted delivery of drugs and imaging labels by overcoming the many biological, biophysical, and biomedical barriers. For in vitro and ex vivo applications, the advantages of state-of-the-art nanodevices (nanochips, nanosensors, and so on) over traditional assay methods are obvious.[8,12] Several barriers exist for in vivo applications in preclinical animal models and eventually clinical translation of nanotechnology, among which are the biocompatibility, in vivo kinetics, targeting efficacy, acute and chronic toxicity, and cost-effectiveness. In this Review, we will summarize the current state-of-the-art of nanoplatforms for targeted molecular imaging in living subjects.
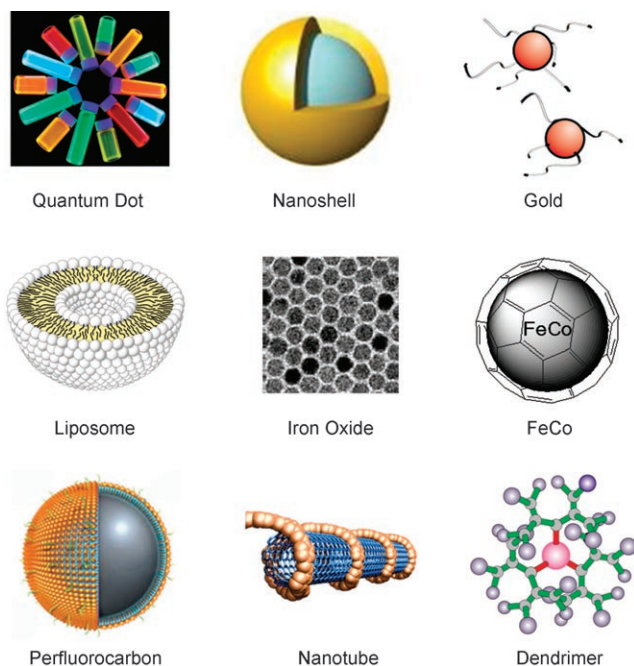
Figure 1. Representative nanoparticles that can serve as nanoplatforms for targeted molecular imaging in living subjects.

[*] Dr. W. Cai, Prof. X. Chen
     Molecular Imaging Program at Stanford (MIPS)
     Department of Radiology and Bio-X Program
     Stanford University, Stanford, CA 94305 (USA)
     Fax: (+1) 650-736-7925
     E-mail: shawchen@stanford.edu

2. Molecular Imaging

Molecular imaging refers to the characterization and measurement of biological processes at the cellular and/or molecular level.[13,14] It can give whole-body readout in an intact system, dramatically decrease the workload and reduce the cost of biomedical research and drug development, provide more statistically relevant results since longitudinal studies can be performed in the same animals, aid in early lesion detection in patients and patient stratification, and help in individualized treatment monitoring and dose optimization.[15] Molecular imaging modalities include optical bioluminescence, optical fluorescence, targeted ultrasound, molecular magnetic resonance imaging (MRI), magnetic resonance spectroscopy (MRS), single-photon-emission computed tomography (SPECT), and positron emission tomography (PET).[14] Many hybrid systems that combine two or more of these modalities are already commercially available and a few others are under active development.[16–18] Although computed tomography (CT) is generally not considered as a molecular imaging modality, the use of nanoparticles as CT contrast agents will be included in this Review.

The use of a molecularly targeted nanoplatform affords many advantages over conventional approaches. First, hundreds, thousands, or even more imaging labels or a combination of labels for different imaging modalities can be attached to a single nanoparticle, which can lead to dramatic signal amplification. Second, multiple, potentially different, targeting ligands on the nanoparticle can provide enhanced binding affinity and specificity. Third, the ability to integrate a means to bypass biological barriers can enable enhanced targeting efficacy. Ultimately, the combination of different targeting ligands, imaging labels, therapeutic drugs, and many other agents may allow for effective and controlled delivery of therapeutic agents in patients, which can be noninvasively monitored in real time. With continuous efforts by multidisciplinary approaches, the use of nanoplatform will shed new light on molecular diagnostics and molecular therapy.

Nanoparticles usually suffer from poorer extravasation when compared to small molecules or proteins. Thus, the majority of naoplatform-based research is so far limited to vasculature-related diseases. In the context of cancer, nanoparticles may also be delivered to tumors through passive targeting mechanisms based on enhanced permeability and retention (EPR) effects.[19,20] This Review will focus on targeted molecular imaging, and the passive targeting of nanoplatforms will only be briefly mentioned where appropriate.

3. Optical Imaging

Optical imaging is a relatively low-cost method suitable primarily for small-animal studies. In fluorescence imaging, excitation light illuminates the subject and the emission light is collected at a shifted wavelength.[21] The major disadvantage of fluorescence imaging is that it is typically not quantitative and the image information is surface-weighted due to tissue absorption.[13] In most cases, significant background signal is also observed because of tissue autofluorescence. A few recently developed techniques such as spectral imaging, where fluorescence signals can be separated based on the emission spectra of different fluorophores,[22,23] and fluorescence-mediated tomography[24,25] can significantly help interpreting the fluorescence imaging data.

3.1. Quantum Dots

The most widely studied nanoparticles for optical imaging applications are quantum dots. QDs are inorganic fluorescent semiconductor nanoparticles with many superior properties for biological imaging than organic fluorophores, such as high quantum yields, high molar extinction coefficients, strong resistance to photobleaching and chemical degradation, continuous absorption spectra spanning UV to near-infrared (NIR; 700–900 nm), long fluorescence lifetimes (> 10 ns), narrow emission spectra (typically 20–30 nm full width at half maximum), and large effective Stokes shifts.[26–28] Numerous in vitro and cell-based applications have been discovered for QDs.[29–31] QDs also have a size-dependent two-photon absorption cross section as high as 47 000 Goeppert–Mayer units, two to three orders of magni-

Xiaoyuan Chen graduated from Nanjing University (P.R. China) with a B.S. degree in chemistry in 1993 and an M.S. degree in 1996. He earned his Ph.D. in chemistry at the University of Idaho in 1999. After that he completed two postdoctoral positions at Syracuse University and Washington University in St. Louis. After briefly working in the peptide industry, he became an assistant professor in the Department of Radiology at the University of Southern California in 2002. He joined the Molecular Imaging Program at Stanford University (MIPS) in 2004 and focuses on the development of multifunctional probes for multimodality molecular imaging.

Weibo Cai was born in P.R. China in 1975. He received his B.S. degree in chemistry from Nanjing University in 1995. He obtained his Ph.D. in chemistry in 2004 from the University of California, San Diego under the guidance of Prof. M. Goodman. He is currently a postdoctoral scholar in Professor X. Chen's group in the Molecular Imaging Program at Stanford University. His research interests are in developing multimodality molecular imaging probes for disease diagnosis and monitoring the therapeutic efficacy of molecular medicine.

tude larger than those of conventional fluorescent probes.[32,33] Since the product of the nonlinear two-photon absorption cross section and the fluorescence quantum yield provides a direct measure of brightness for imaging,[34] QDs are ideal probes for multiphoton microscopy in live animals. Modeling studies have revealed that two spectral windows exist for optimal QD-based imaging in living subjects, one at 700–900 nm and the other at 1200–1600 nm.[35] For in vivo applications, non-targeted QDs have been reported for cell trafficking,[36–38] vasculature imaging,[33,39,40] sentinel lymph node mapping,[41–44] and neural imaging.[45,46]

In order to make QDs more useful for biomedical applications, QDs need to be effectively, specifically, and reliably directed to a specific organ or disease site without alteration. Specific targeting can be achieved by attaching targeting molecules to the QD surface. However, in vivo targeting and imaging is very challenging due to the relatively large overall size (typically >20 nm in hydrodynamic diameter) and short circulation half lives of QD conjugates. To date, there have been only a handful of successful reports in the literature.

U87MG human glioblastoma tumors, where tumor fluorescence intensity reached maximum at 6 h post injection (Figure 2).[48] The size of QD705-RGD ($\approx$20 nm in diameter) prevented efficient extravasation, thus QD705-RGD mainly targeted tumor vasculature instead of tumor cells as confirmed by ex vivo immunofluorescence staining. As the
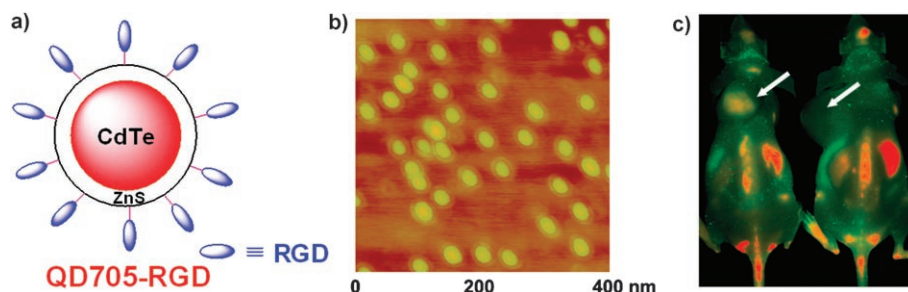

Figure 2. RGD peptide-conjugated QD705 for NIRF imaging of tumor vasculature. a) A schematic illustration of the probe QD705-RGD. b) An atomic force microscopy image of QD705-RGD deposited on a silicon wafer. c) In vivo NIRF imaging of tumor vasculature in U87MG human glioblastoma-tumor-bearing mice. The mouse on the left was injected with QD705-RGD and the mouse on the right was injected with QD705. Arrows indicate tumors (adapted from Ref. [48]).

sprouting neovasculature in many tumor types overexpresses integrin $\alpha_v\beta_3$, QD705-RGD has great potential as a universal NIRF probe for detecting tumor vasculature in living subjects.

3.3. Antibody-Conjugated Quantum Dots

QDs have been conjugated to prostate specific membrane antigen (PSMA)-specific monoclonal antibodies for prostate cancer targeting and imaging in mice.[53] Multiplexed imaging was also demonstrated using various QD-labeled cancer cells. In this study, both passive targeting and active targeting mechanisms were investigated using QDs with different surface ligands. Since no histological analysis was carried out to investigate PSMA expression on the tumor cells and tumor vasculature, it was unclear whether these QD conjugates targeted the tumor vasculature or tumor cells. In a recent study, QDs were linked to an anti-AFP (alpha-fetoprotein, a marker for hepatocellular carcinoma cell lines) antibody for in vivo tumor imaging.[54] Using an integrated fluorescence imaging system, spectroscopic hepatoma imaging was achieved and the heterogeneous distribution of the QD-based probe in the tumor was also evaluated by a site-by-site measurement method. The major flaw of this study is that it was not shown whether or not the anti-AFP antibody was actually linked to the QD. Therefore, there is not enough experimental evidence to support the conclusion that the tumor contrast observed was from active, rather than passive, targeting.

Tracking the movement of a single QD–antibody conjugate (total number of QD particles injected was $\approx 1.2 \times 10^{14}$) inside the tumor through a dorsal skinfold chamber was recently accomplished using a high-speed confocal microscope with a high sensitivity camera.[55] This technique was able to

3.2. Peptide-Conjugated Quantum Dots

Specific targeting of QD conjugates in living subjects was first reported using peptides as the targeting ligands.[47] In this pioneering study, ex vivo histological analysis showed that QDs were specifically directed to the tumor vasculature and other targets by different peptides. Although no in vivo imaging was achieved, this study demonstrated the feasibility of using QD as a nanoplatform for in vivo specific targeting, which opened up a new field of QD-based research. Recently, Cai et al. reported the in vivo targeted imaging of tumor vasculature using peptide-conjugated QDs.[48] Integrin $\alpha_v\beta_3$, a cell adhesion molecule, is overexpressed on activated endothelial cells and tumor cells but is not readily detectable in resting endothelial cells and most normal organ systems.[49] Many previous reports have demonstrated that integrin $\alpha_v\beta_3$ is an excellent target for imaging purposes.[50–52] The fact that integrin $\alpha_v\beta_3$ is expressed on both tumor vasculature and tumor cells makes it a prime target for nanoplatform-based imaging, as extravasation is not required to observe tumor signal. In this study, arginine-glycine-aspartic acid (RGD; potent integrin $\alpha_v\beta_3$ antagonist) containing peptides were conjugated to QD705 (emission maximum at 705 nm) and QD705-RGD exhibited high affinity integrin $\alpha_v\beta_3$ specific binding in cell culture and ex vivo. In vivo NIR fluorescence (NIRF) imaging was successfully achieved in nude mice bearing subcutaneous integrin $\alpha_v\beta_3$-positive

capture the specific delivery of a single QD particle entering into circulation, extravasating into the interstitial space from the vasculature, binding to the tumor cell surface receptor, and reaching the perinuclear region after traveling on the intracellular rail protein. However, this study did not provide any information regarding the percentage of intravenously injected QDs that extravasated. Thus, little can be concluded about the overall behavior of such QD–antibody conjugates in vivo. Whether the described delivery pattern is typical for the majority of injected QD conjugates, or if it is only limited to a very small subset of QDs, remains to be elucidated in the future.

QD-based fluorescence imaging in small animals can not be directly scaled up to in vivo imaging in patients due to the limited optical signal penetration depth. In clinical settings, optical imaging is relevant for tissues close to the surface of the skin, tissues accessible by endoscopy, and during intraoperative visualization. QD-based imaging may play an important role in image-guided surgery in the future. The major roadblocks for clinical translation of QDs are inefficient delivery, potential toxicity, and lack of quantification.[31] However, with the development of smaller,[42,56] less toxic,[43,57] multifunctional[58,59] QDs and further improvement of the conjugation strategy, it is expected that QDs may achieve optimal tumor targeting efficacy with acceptable toxicity profile for clinical translation in the near future.

3.4. Other Nanoparticles

Optical coherence tomography (OCT) is an imaging technique with high resolution (typically 10–15 μm), which can allow for real-time, cross-sectional imaging through biological tissues.[60,61] OCT detects the reflection of a low-coherence light source directed into a tissue and determines at what depth the reflections occurred. Nanoshells[62,63] and gold nanocages[64] have been reported for OCT imaging in vitro. The surface plasmon resonance properties of these nanoparticles make them promising both as contrast agents for in vivo optical imaging, and as therapeutic agents for photothermal treatment of diseases.[65] Although having great potential, efficient targeted delivery of these nanoparticles in vivo, a goal central to any potential therapeutics, has not been demonstrated. Much future effort is needed to evaluate the fate and biological effects of such nanoparticles in animals before any biomedical applications can be in place. In another study, ligand-conjugated, NIR-labeled low-density lipoprotein (LDL) nanoparticles that enable the in vivo demonstration of rerouting LDL from LDL receptors to selected alternate receptors were recently reported.[66] This approach may expand the range of using LDL particles as nanoplatforms for in vivo cancer imaging and treatment.

4. Computed Tomography

CT is a medical imaging method where digital geometry processing is used to generate a 3D image of the internals of an object from a large series of two-dimensional X-ray images taken around a single axis of rotation.[67] CT is not a molecular imaging modality yet due to the lack of target-specific contrast agents. Current CT contrast agents are typically based on iodine and gadolinium-based molecules, which have mostly nonspecific distribution and rapid pharmacokinetics.[68,69] Iodinated nanoparticles have also been reported as CT contrast agents.[70–75] Recently, detection of macrophages in atherosclerotic plaques of rabbits, following intravenous injection of a contrast agent formed of iodinated nanoparticles dispersed with surfactant, was achieved with a clinical CT scanner (Figure 3).[76] This contrast agent may become an important adjunct to the clinical evaluation of coronary arteries with CT.
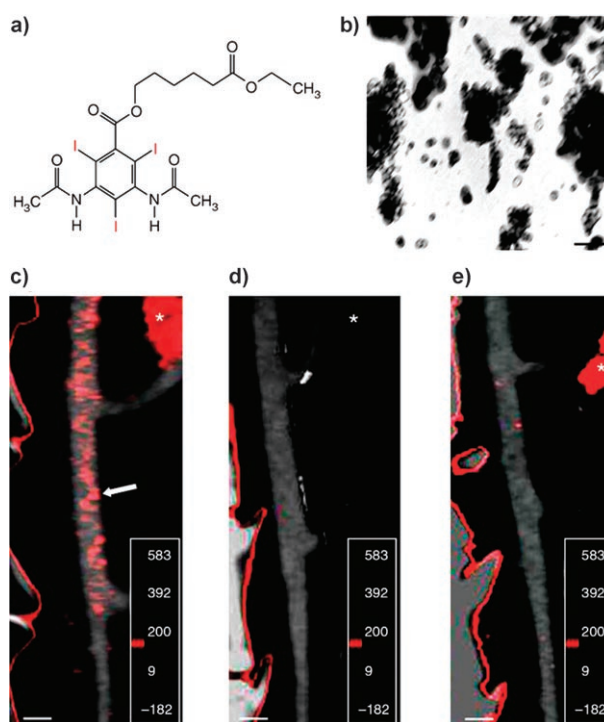

Figure 3. Nanoparticles as CT contrast agents. a) Chemical structure of the iodinated CT contrast agent with the three iodine atoms in red. b) Electron microscopy image of the iodinated nanoparticles after staining with a solution of uranyl acetate. Bar width: 100 nm. c) Significant contrast was observed in atherosclerotic plaques (arrow) after injection of iodinated nanoparticles. d) No appreciable contrast was observed in atherosclerotic plaques after injection of a conventional contrast agent. e) No appreciable contrast was observed in the aortic wall of a control animal injected with the iodinated nanoparticles. Scale bar: 5 mm (adapted from Ref. [76]).

To date, all contrast-enhanced CT imaging are based on nonspecific targeting and no molecular CT has been reported. A polymer-coated Bi_2S_3 nanoparticle (10–50 nm per side, 3–4 nm thick) was recently reported as an injectable CT contrast agent.[77] With more than a fivefold increase in X-ray absorption than iodine, very long circulation times (>2 h) in vivo, and an efficacy/safety profile comparable to or better than iodinated contrast agents, these nanoparticles and their bioconjugates may potentially be used for CT

imaging of molecular targets and pathological conditions. Because of the ubiquitous nature of CT in the clinical setting, as well as the increasing use and development of microCT and hybrid systems that combine PET or SPECT with CT, molecular CT will likely become a reality in the near future.

5. Targeted Ultrasound

Because of its safety, low cost, ease of use, and wide availability, ultrasonography is the most commonly used clinical imaging modality.[78] High-frequency sound waves are emitted from a transducer placed against the skin and ultrasound images are obtained based on the sound wave reflected back from the internal organs. The contrast of ultrasound is dependent on the sound speed, sound attenuation, backscatter, and the imaging algorithm.[79]

Ultrasound contrast agents have been used in the clinic for applications such as blood pool enhancement, characterization of liver lesions, and perfusion imaging.[80,81] These contrast agents are generally in the form of small acoustically active particles ranging from several hundred nanometers to a few micrometers in diameter. Microbubbles resonate in an ultrasound beam, rapidly contracting and expanding in response to the pressure changes of the sound wave, thus leading to enhanced ultrasound contrast.[82] Targeting is accomplished either through manipulating the chemical properties of the microbubble shell or through conjugation of disease-specific ligands to the microbubble surface.[78,83] As these microbubbles are too large to extravasate, the disease process must be characterized by molecular changes in the vascular compartment to be imaged. Integrin $\alpha_v\beta_3$ and vascular endothelial growth factor receptor 2 (VEGFR-2; Flk-1/KDR) targeted ultrasound have been reported using ligand-conjugated microbubbles.[84–88]

Ligand-coated perfluorocarbon (PFC) emulsion nanoparticles (≈ 250 nm in diameter) were used to identify the angioplasty-induced expression of tissue factor by smooth muscle cells within the tunica media (Figure 4).[89,90] Pig carotid arteries were overstretched bilaterally with balloon catheters, treated with a tissue factor-targeted or a control nanoparticle system, and imaged with intravascular ultrasound (20 MHz) before and after treatment. Tissue factor-targeted nanoparticles bound to and increased the echogenicity of tissue factor expressing smooth muscle cells within the tunica media. The area of acoustic enhancement also appeared to coincide with the expression of induced tissue factor as revealed by immunohistochemistry. Detection of neovasculature in tumors implanted in athymic nude mice has also been achieved using a research ultrasound scanner after injection of targeted PFC nanoparticles.[91]

Ultrasound has relatively high spatial resolution (typically < 500 μm) yet it also has some disadvantages such as relatively poor depth penetration (usually a few centimeters depending on the frequency used) and limited sensitivity.[14] Due to the large size of the contrast agents used (usually > 200 nm), the molecular targets are exclusively vasculature related. Disruption of the microbubbles or nanoparticles
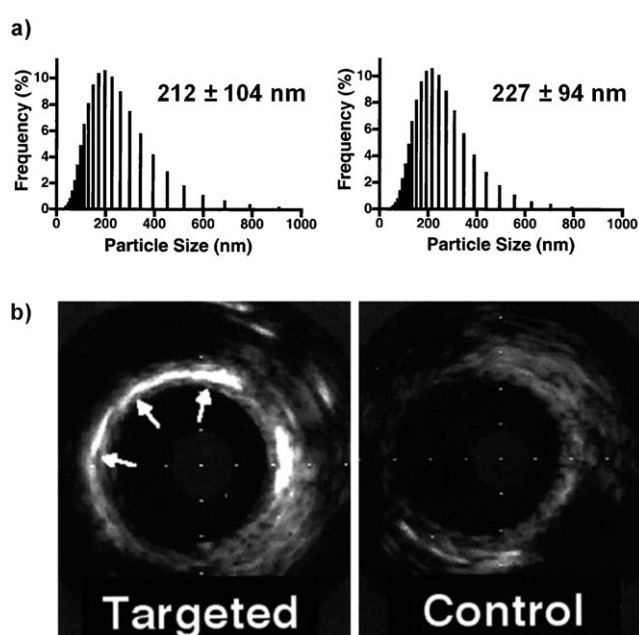

Figure 4. Nanoparticles for targeted ultrasound imaging. a) Particle size distribution of tissue factor-targeted perfluorocarbon nanoparticles (left) and unconjugated control nanoparticles (right). b) High-frequency intravascular ultrasonic images of carotid arteries exposed to tissue factor-targeted or control nanoparticles after angioplasty (adapted from Refs. [89,90]).

after reaching the targeted vasculature may potentially be employed for targeted delivery of therapeutic agents.

6. Molecular MRI

MRI is a noninvasive diagnostic technique based on the interaction of certain nuclei (typically protons) with each other and with surrounding molecules in a tissue of interest.[92] Different tissues have different relaxation times, which can result in endogenous contrast. Exogenous contrast agents can further enhance this by selectively shortening either the T1 (longitudinal) or T2 (transverse) relaxation time.[93,94] The MR image can be weighted to detect differences in either T1 or T2 by adjusting parameters during data acquisition. Traditionally, gadolinium chelates have been used to increase the T1 contrast.[95] Recently, novel MR contrast agents with significantly higher relaxivities have been reported, such as paramagnetic gadolinium-containing liposomes/micelles and superparamagnetic iron oxide (SPIO) nanoparticles.[6,93] The major advantages of MRI over radionuclide-based imaging are the absence of radiation and higher spatial resolution (usually sub-millimeter level). The disadvantage of MRI is its inherent low sensitivity, which can only be partially compensated by working at higher magnetic fields (4.7–14 T), acquiring data for much longer periods during imaging, and using exogenous contrast agents.

6.1. Non-Targeted MR Contrast Agents

Iron oxide nanoparticles are the most widely used nanoparticle-based MR contrast agents. Since nanoparticles are usually nonspecifically taken up by the reticuloendothelial system (RES)[96] and the overall size of the nanoparticle can affect which organ (liver, spleen, or lymph node) they go to, non-targeted iron oxide nanoparticles have been used for liver,[97,98] spleen,[99,100] and lymph node imaging.[101,102] These nanoparticles can also accumulate at the tumor site due to the presence of leaky vasculature (the extent of extravasation depends on the porosity of the angiogenic tumor vessels) as well as from macrophage uptake.[103–105] The role of macrophages in pathologic tissue alterations in the central nervous system has led to the use of SPIO agents for imaging of stroke,[106] multiple sclerosis,[107] brain tumors,[108] and carotid atherosclerotic plaques.[109] Iron oxide nanoparticles can be detected at quite low concentration and single-cell or single-particle detection has been reported.[110–112] Thus, iron oxide nanoparticles have recently been used to label cells and track their biodistribution and migration in vivo with MRI.[113–117]

Recently, FeCo/single-graphitic-shell nanoparticles that are soluble and stable in aqueous solutions were reported.[118] The nanoparticles exhibit ultrahigh saturation magnetization and r1/r2 relaxivities. Preliminary in vivo experiments demonstrated long-lasting positive-contrast enhancement for vascular MRI in rabbits (Figure 5). These nanoparticles may have the potential for integrated diagnosis and therapeutic (photothermalablation) applications.

6.2. Molecular MRI of Integrin $\alpha_v\beta_3$ Expression

Integrin $\alpha_v\beta_3$ is the most well-studied target for molecular MRI.[15,119,120] Antibody-coated paramagnetic liposomes (300–350 nm in diameter) containing Gd^{3+} ions were first reported for MRI of integrin $\alpha_v\beta_3$ expression.[121] In this study, molecular MRI of squamous cell carcinomas in a rabbit model was achieved by targeting paramagnetic liposomes to the angiogenic vasculature using LM609, a mouse anti-human integrin $\alpha_v\beta_3$ monoclonal antibody. Site-directed

contrast enhancement of angiogenic vessels in a rabbit corneal micropocket model has also been reported using antibody-coated Gd^{3+}–PFC nanoparticles (400–700 nm in diameter).[122]

Peptidomimetic integrin $\alpha_v\beta_3$ antagonist was conjugated to magnetic nanoparticles for molecular MRI under a common clinical field strength of 1.5 T.[123,124] In a Vx-2 squamous cell carcinoma model, integrin $\alpha_v\beta_3$-targeted paramagnetic nanoparticles increased the MR signal dramatically in the periphery of the tumor at 2 h post injection.[123] Despite the relatively large size ($\approx$270 nm in diameter), these nanoparticles penetrated into the leaky tumor neovasculature but did not migrate into the interstitium in appreciable amounts. In an atherosclerosis model, enhancement in MR signal was also observed among rabbits that received targeted nanoparticles.[124] In a later study, athymic nude mice bearing human melanoma tumors were successfully imaged using systemically injected $\alpha_v\beta_3$ integrin-targeted paramagnetic nanoparticles.[125]

Recently, integrin $\alpha_v\beta_3$-targeted paramagnetic nanoparticles were reported for noninvasive assessment of angiogenesis in early atherosclerosis, for site-specific delivery of an antiangiogenic drug (fumagillin, an antibiotic which can block blood vessel formation by binding to methionine aminopeptidase 2), and for quantitative follow-up of the therapeutic response (Figure 6).[126] Seven days after a single treatment with $\alpha_v\beta_3$-targeted nanoparticles with or without fumagillin, the targeted nanoparticles were readministered and decreased MR contrast enhancement was observed among the treated animals but not in control animals. Ex vivo histological analysis was also carried out to confirm the in vivo results. This study demonstrated the potential of combining molecular imaging and drug delivery with targeted nanoparticles to noninvasively define the atherosclerotic burden, to monitor the drug delivery, and to quantify local response to treatment.

6.3. Molecular MRI of Other Targets

Fibrin-targeted Gd^{3+}-containing nanoparticles were assessed in dogs under open-circulation conditions.[127] It was demonstrated that fibrin-targeted paramagnetic nanoparticles can provide sensitive detection and localization of fibrin, which may allow for early identification of vulnerable plaques and lead to early therapeutic decisions. The concept of vascular smooth muscle cell (VSMC)-targeted nanoparticles as a drug-delivery platform for the prevention of restenosis after angioplasty has been studied.[128] Tissue factor-targeted nanoparticles containing doxorubicin or paclitaxel
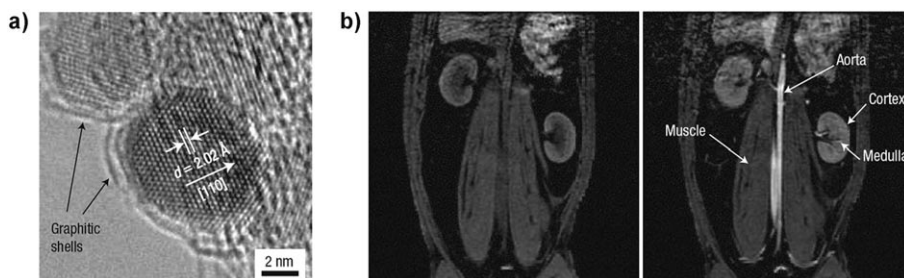

Figure 5. FeCo/graphitic-shell nanoparticles for MRI applications. a) A high-resolution transmission electron microscopy image of two FeCo nanoparticles, each with a graphitic shell. b) T1-weighted MR images of a rabbit before (left) and 30 min after (right) injection of the FeCo/graphitic-shell nanoparticles. The blood pool in the aorta is significantly brightened in the MRI after injection. Signal increase in the kidney medulla and cortex was also observed due to the high blood volume within the kidney (adapted from Ref [118]).
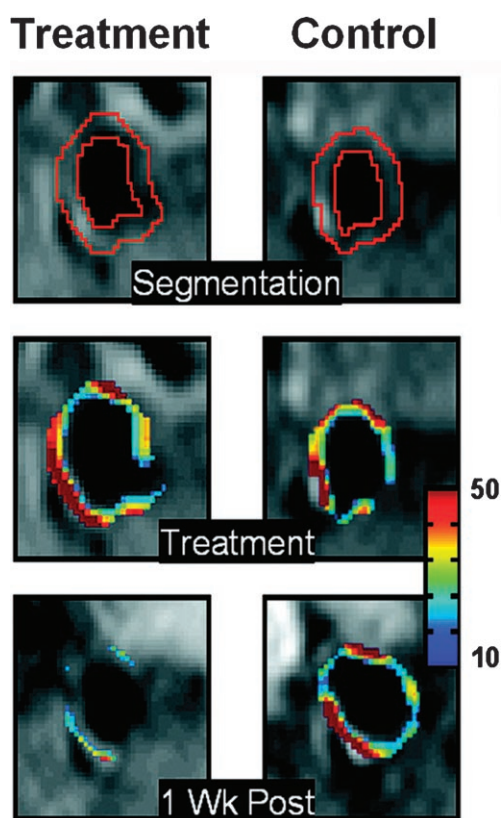
Figure 6. MRI of the rabbit abdominal aorta showing outline of segmented region-of-interest (top), false-colored overlay of percent signal enhancement at time of treatment (middle), and one week post-treatment (bottom) with integrin $\alpha_v\beta_3$-targeted nanoparticles with or without fumagillin, an anti-angiogenic antibiotic (adapted from Ref. [126]).

(both are chemotherapeutic drugs for treating a wide range of cancers) were found to significantly increase the anti-proliferative effectiveness. Nanoparticles adherent to the VSMC were detected with high-resolution T1-weighted MRI at 4.7 T and ^{19}F-MRS of the nanoparticle core also enabled quantitative and noninvasive dosimetry evaluation of targeted drug payloads.

Latex nanoparticles of different sizes have been derivatized with tomato lectin (a very stable glycoprotein that effectively binds to blood vessels in rodents) and Gd^{3+} chelates for vasculature contrast enhancement in MRI.[129] A nanoparticle agent based on high-density lipoproteins (HDL) was used for the MR detection of atherosclerotic plaques in vivo.[130] A multifunctional nanoplatform that contains MRI and photodynamic therapy (PDT) agents inside, as well as targeting ligands on the surface, has been developed and exhibited improved MR contrast enhancement and PDT efficacy.[131]

Through a process that involved systematic evaluation of the magnetic spin, size, and type of spinel metal ferrites, Mn-doped magnetism-engineered iron oxide (MnMEIO) conjugated with trastuzumab (an anti-HER2 monoclonal antibody) were recently shown to be able to visualize small HER2-positive tumors implanted in mice while trastuzu-

mab-conjugated cross-linked iron oxide (CLIO) did not.[132,133] Since both CLIO and MnMEIO were conjugated to trastuzumab to the same extent based on fluorescent-activated cell sorting (FACS) analysis, the absence of tumor contrast enhancement for CLIO–trastuzumab was attributed to two main factors: the larger size of CLIO, which prevents efficient extravasation, and its lower magnetic property, which renders it not readily detectable by MRI at low concentration.

Molecular MRI is still in its infancy. In many of the studies, ex vivo histology was not carried out to investigate/validate whether the targeted MR contrast agents are targeting the tumor vasculature, targeting the tumor cells, or accumulating nonspecifically in the interstitial space. It is likely that the feasible targets reachable by these ligand-targeted paramagnetic nanoparticles will be mostly vasculature related, as the overall size of iron oxide nanoparticles with surface polymer coating and targeting ligands are usually quite large (>20 nm in diameter). Newly developed nanoparticles with smaller sizes (preferably <20 nm in diameter) and long circulation half life (at least a few hours) may allow for extravasation from the leaky tumor vasculature to a certain extent. Surface coating of these nanoparticles with small molecules or peptides should have better targeting efficacy than antibody-coated nanoparticles, because of the much higher number of targeting ligands and significantly smaller overall size. As the major disadvantage of MRI is its inherent low sensitivity, future development of novel contrast agents with the capability of targeting the cells in addition to the vasculature may dramatically increase the MR signal and facilitate the biomedical applications of molecular MRI.

7. Radionuclide-Based Imaging

Radionuclide-based imaging includes SPECT and PET, where internal radiation is administered through a low mass amount of pharmaceutical labeled with a radioisotope.[14] The major advantages of radionuclide-based molecular imaging are that they are very sensitive, quantitative, and there is no tissue penetration limit. The disadvantage is that the resolution (typically >1 mm) of either SPECT or PET is not as high as the other imaging modalities. In most cases, the purpose of labeling the nanoparticle with a radionuclide was for the noninvasive evaluation of its pharmacokinetic properties with SPECT or PET.

7.1. Nanoplatform for SPECT Imaging

The source of SPECT images are gamma-ray emissions.[134,135] The radioisotope decays and emits gamma rays, which can be detected by a gamma camera to obtain 3D images. The first object that an emitted gamma photon encounters after exiting the body is the collimator, which allows it to travel only along certain directions to reach the detector, to ensure that the signal position on the detector accurately represents the source of the gamma ray. Because of the use of collimators to define the angle of incidence,

SPECT imaging has a very low detection efficiency (typically $<10^{-4}$ times the emitted number of gamma rays).[14]

The pharmacokinetics, tumor uptake, and therapeutic efficacy of an ^{111}In ($t_{1/2}$: 2.8 days)-labeled chimeric L6 (ChL6) monoclonal antibody-linked iron oxide nanoparticle was studied in athymic mice bearing human breast cancer HBT 3477 tumors.[136] ^{111}In-labeled ChL6 was conjugated to carboxylated polyethylene glycol (PEG) on dextran-coated iron oxide nanoparticles (≈ 20 nm in diameter), with one to two ChL6 antibodies per nanoparticle (Figure 7). It was pro-
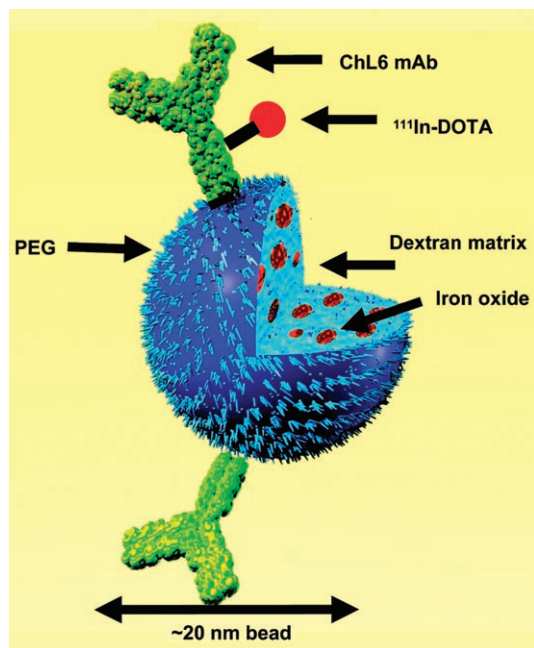

Figure 7. ^{111}In-labeled ChL6 antibody was conjugated to a 20 nm dextran bead coated with polyethylene glycol and impregnated with iron oxide. Such a nanoplatform can enable tumor-specific thermal therapy through external application of an alternating magnetic field (reprinted with permission from Ref. [137]).

posed that the time this nanoparticle remained in the circulation was long enough to provide ample opportunity for it to exit the blood vessels and access the cancer cells. Inductively heating the nanoparticle with an externally applied alternating magnetic field (AMF) caused tumor necrosis at 24 h after AMF therapy. In a follow-up study, different doses of AMF were delivered at 72 h after nanoparticle injection.[137] SPECT imaging was carried out to quantify the nanoparticle uptake in the tumor, which was about 14 percentage injected dose per gram (%ID/g) at 48 h post-injection. Delay in tumor growth occurred after AMF treatment and the difference was found to be statistically significant when compared with the untreated group.

Integrin $\alpha_v\beta_3$-targeted ^{111}In-labeled PFC nanoparticles were reported for the detection of tumor angiogenesis in New Zealand white rabbits implanted with Vx-2 tumors.[138] Nanoparticles bearing approximately 10 ^{111}In atoms per particle had better tumor-to-muscle ratio than those with only approximately one ^{111}In atom per particle. At 18 h after injection, mean tumor activity in rabbits receiving integrin

$\alpha_v\beta_3$-targeted nanoparticles was about four times higher than the non-targeted control. The spleen was found to be the primary clearance organ based on biodistribution studies.

The major advantage of SPECT imaging over PET is that it can potentially allow for simultaneous imaging of multiple radionuclides, since the gamma rays emitted from different radioisotopes can be differentiated based on the energy.[139] However, no dual radioisotope imaging of radiolabeled nanoparticles has been reported and whether it can provide a significant advantage over single-isotope SPECT remains to be tested. Over the last decades, PET imaging has become more and more popular in both preclinical and clinical settings.

7.2. Nanoplatform for PET Imaging

PET uses positron emitter-labeled molecules in very low mass amounts to image and measure the function of biological processes with minimal disturbance.[140,141] The sensitivity of PET is significantly higher than SPECT since no collimator is used. With the development of microPET scanners dedicated to small-animal imaging studies (which can provide a similar in vivo imaging capability in mice, rats, and monkeys), one can readily transfer knowledge and molecular measurements between species, which can facilitate clinical translation of newly developed PET agents.[142,143] To date, there have been very few reports on PET imaging of targeted nanoparticles.

Single-walled carbon nanotubes (SWNTs) exhibit unique size, shape, and physical properties that make them promising candidates for biological applications.[3,4] Liu et al. investigated the biodistribution of ^{64}Cu ($t_{1/2}$: 12.7 h)-labeled SWNTs in mice by PET, ex vivo biodistribution, and Raman spectroscopy (Figure 8).[144] It was found that these SWNTs are surprisingly stable in vivo and the surface PEG chain length can significantly affect the biodistribution and circulation half-life. Effectively PEGylated SWNTs exhibit relatively long circulation half life (about 2 h) and low uptake by the RES. Efficient targeting of integrin $\alpha_v\beta_3$-positive tumors in mice was achieved with SWNTs coated with PEG chains linked to cyclic RGD peptides. The Raman signatures of SWNTs were also used to directly probe the presence of SWNTs in mice tissues and confirm the radionuclide-based imaging results. After evaluating the pharmacokinetics and tumor-targeting efficacy, the use of SWNTs as a nanoplatform for integrated multimodality imaging and molecular therapy is currently in progress.

Radionuclide-based imaging has much higher sensitivity than MRI and much better tissue penetration than optical imaging and ultrasound. The most important advantage of radionuclide-based imaging over other imaging modalities is the ability to quantitatively measure the radionuclide concentration in various organs over time, which can provide invaluable information about the pharmacokinetics and the full-body distribution of the radio-labeled nanoparticles. Different from other molecular imaging modalities where typically the nanoparticle itself is detected, radionuclide-
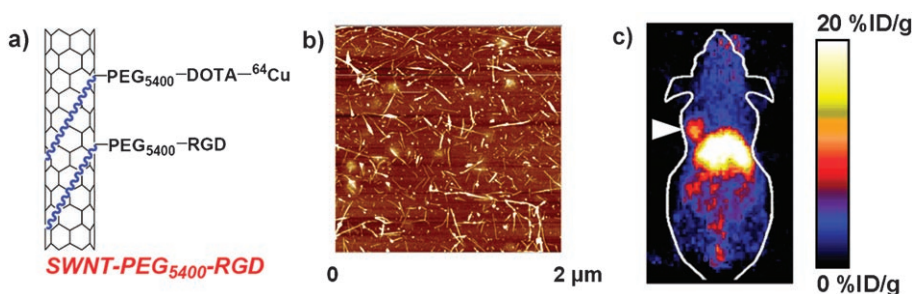
Figure 8. Single-walled carbon nanotubes (SWNTs) as nanoplatforms for in vivo tumor targeting and imaging. a) Schematic illustration of a noncovalently functionalized SWNT. The hydrophobic chains (blue segments) of the phospholipids bind strongly to the sidewall of the SWNT, and the PEG chains render water solubility. RGD peptide can allow for integrin $\alpha_v\beta_3$ targeting and DOTA molecules on the SWNT can complex ^{64}Cu for PET imaging. b) An atomic force microscopy image of the SWNT deposited on a silicon substrate. c) A 2D projection microPET image of a mouse bearing an integrin $\alpha_v\beta_3$-postive tumor at 8 h post-injection of the RGD- and ^{64}Cu-containing SWNT. The arrow indicates the tumor (adapted from Ref. [144]).

based imaging detects the radiolabel rather than the nanoparticle. The nanoparticle distribution is measured indirectly by assessing the localization of the radionuclide. Dissociation of the radionuclide (typically metal) from the chelator and/or the radionuclide-containing polymer coating from the nanoparticle may occur, which can cause significant differences between the nanoparticle distribution and the radionuclide distribution. Thus, the stability of the radiolabel on the nanoparticle should be rigorously evaluated and the distribution of the nanoparticle itself should also be measured to confirm the radionuclide-based imaging results, as demonstrated in the above-mentioned study. With advances in nanotechnology and more robust bioconjugation chemistry, radio-labeled nanoplatforms deserve significant research efforts as they can allow for the ultimate integration of quantitative, noninvasive imaging and targeted molecular therapy within one entity.

8. Multimodality Imaging

Among all molecular imaging modalities, no single modality is perfect and sufficient to obtain all the necessary information.[14] For example, it is difficult to accurately quantify fluorescence signals in living subjects, particularly in deep tissues; MRI has high resolution yet it suffers from low sensitivity; Radionuclide-based imaging techniques have very high sensitivity but they have relatively poor resolution. The combination of multiple molecular imaging modalities can offer synergistic advantages over any modality alone. Combining optical imaging with 3D tomographic techniques such as PET, SPECT, or MRI can allow for noninvasive imaging in living subjects with higher sensitivity and/or accuracy. Multimodality imaging using a small-molecule-based probe is very challenging due to the limited number of attachment points and the potential interference with its receptor binding affinity. On the other hand, nanoparticles have large surface areas where multiple functional moieties can be incorporated for multimodality molecular imaging.

Dual-modality nanoplatform-based probes for both MR and optical imaging have been reported. MR-detectable and fluorescent liposomes carrying RGD peptides were investigated for in vivo tumor imaging.[145] Both RGD-conjugated liposomes and RAD (a control peptide that does not bind integrin $\alpha_v\beta_3$)-conjugated liposomes gave enhanced T1-weighted MR contrast. Using ex vivo fluorescence microscopy, it was found that RGD-conjugated liposomes were specifically associated with the activated tumor endothelium while RAD-conjugated liposomes were located in the extravascular compartment. CLIO nanoparticles have been loaded with fluorescent dyes (e.g., Cy5.5), either via an enzyme-cleavable linker[146] or with additional targeting ligands such as antivascular cell adhesion molecule (VCAM)-1 antibodies[147] or E-selectin-binding peptides.[148] In both studies, in vivo NIRF imaging was carried out, yet noninvasive MRI was not achieved likely due to the low sensitivity. In other reports, similar nanoparticles were linked with VCAM-1 binding peptides,[149,150] bombesin peptides,[151] or annexin V (a 35 kDa Ca^{2+}-dependent protein with high affinity for phosphatidylserine, which translocates from the inner to the outer leaflet of the plasma membrane during early stage of apoptosis).[152] In these cases, in vivo MRI was accomplished but in vivo NIRF imaging was not, likely due to the limited tissue penetration of light even in the NIR region. Although only single-modality noninvasive imaging was achieved with these dualmodality probes, which does not take full advantage of the nanoplatform-based approach, the capability of detecting the probe with another imaging modality did provide a convenient way for ex vivo validation, which is more reliable and advantageous than the single-modality probes.

Cai et al. recently developed a QD-based probe for both NIRF and PET imaging.[153] QD surface modification with RGD peptides allows for integrin $\alpha_v\beta_3$ targeting and DOTA (1,4,7,10-tetraazacyclododecane-1,4,7,10-tetraacetic acid; a very effective chelator for many metal ions) conjugation enables PET imaging after ^{64}Cu-labeling. Using this dual-modality probe, we quantitatively evaluated the tumor-targeting efficacy and found that the majority of the probe in the tumor was within the tumor vasculature. The PET/NIRF dual-modality probe can confer sufficient tumor contrast detectable by PET at much lower concentration than that required for in vivo NIRF imaging,[48] thus significantly reducing the potential toxicity of cadmium-based QDs, and greatly facilitating their future biomedical applications.[154,155] In another report, liposomes were labeled with both radionuclides and gadolinium for SPECT and MR imaging in vitro.[156] However, in vivo imaging has not yet been achieved.

Most of the above-mentioned studies demonstrated the feasibility of dual-modality imaging in vivo, but the two modalities were not equally effective. The less-sensitive modality was usually used for ex vivo validation of the in vivo results obtained from the more-sensitive imaging modality. It is not until very recently that noninvasive dual-modality imaging was accomplished using a nano-platform-based approach.[157] Gene silencing using short interfering RNA (siRNA) has become an attractive approach to probe gene function in mammalian cells.[158–160] A multifunctional probe for in vivo transfer of siRNA and simultaneous imaging of its accumulation in tumors by both MR and NIRF imaging was reported.[157] This probe consists of magnetic nanoparticles, labeled with an NIR dye, covalently linked to siRNA molecules specific for either model or therapeutic targets. Additionally, the nanoparticle was modified with a membrane translocation peptide for intracellular delivery.[161,162] In vivo tracking of the multifunctional probe in the tumor by MR and NIRF imaging in two tumor models was demonstrated (Figure 9). This study represents the first example of combining noninvasive multimodality imaging and molecular therapy using a nanoplatform-based approach.

Table 1. Nanoplatforms composed of different materials have been reported for biomedical applications using various molecular imaging modalities. Note that some nanoparticles do not possess intrinsic imaging signal, thus the modality depends on the label used in a particular study.

Nanoplatform	Composition	Imaging modality	References
Quantum dot	CdSe, CdTe	optical fluorescence	[47, 48, 53, 55]
Nanoshell, nanocage	gold	OCT	[62–64]
Iodinated nanoparticle	iodine	CT	[70–75]
Bi_2S_3 nanoparticle	Bi_2S_3	CT	[77]
PFC nanoparticle	perfluorocarbon	depends on the label	[89–91, 122–126, 138]
SPIO, CLIO	iron oxide	MRI	[97–117, 146-152]
FeCo nanoparticle	Fe, Co	MRI	[118]
MnMEIO	Mn, iron oxide	MRI	[132, 133]
SWNT	carbon	depends on the label	[144]
Liposome	phospholipid	depends on the label	[121, 145, 156]

both non-targeted MRI and molecular MRI are iron oxide nanoparticles, some of which are already in the clinic and/or in late-stage clinical trials. The use of nanoparticles in the other imaging modalities (CT, ultrasound, and radionuclide-based imaging) is relatively rare. Recently, multifunctional nanoparticles for multimodality molecular imaging have also emerged. PET/optical, MRI/optical, and SPECT/MRI have been demonstrated either in vitro, ex vivo, or in vivo. The future of nanomedicine lies in multifunctional nanoplatforms, which combine both therapeutic components and multimodality imaging. The ultimate goal is that nanoplatform-based agents can allow for efficient, specific in vivo delivery of drugs without systemic toxicity, and the dose delivered as well as the therapeutic efficacy can be accurately measured noninvasively over time. Much remains to be done before this can be a clinical reality and many factors need to be optimized, among which are biocompatibility, pharmacokinetics, in vivo targeting efficacy, cost-effectiveness, and acute/chronic toxicity.

Like most new technologies, there are concerns about the possible side effects derived from the use of nanoparticles. The potential toxicity of nanoparticles mainly comes from two aspects. First, nanoparticles can enter the body through the skin, lungs, or intestinal tract, depositing in several organs and may cause adverse biological reactions. In addition, the toxicity of nanoparticles also depends on whether they get cleared from the body and whether the host can raise an effective response to sequester or dispose of the particles. Second, the toxicity can come from the material itself, such as CdSe/CdTe in QDs. Interestingly, the toxicity of QDs has been utilized for photodynamic therapy applications such as tumor ablation.[163,164] Thick ZnS overcoating (4–6 monolay-
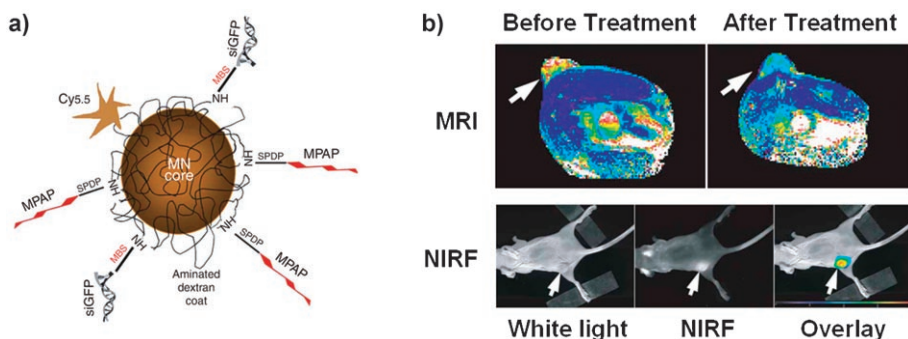

Figure 9. A multifunctional probe for in vivo dual-modality imaging and therapy. a) Schematic illustration of the multifunctional probe consisting of a magnetic nanoparticle labeled with a near-infrared dye Cy5.5, membrane translocation peptides (MPAP), and siRNA molecules targeting green fluorescent protein (siGFP). b) In vivo MRI of mice bearing subcutaneous LS174T human colorectal adenocarcinoma (arrows) before and after treatment. A high-intensity NIRF signal in the tumor confirmed the delivery of the nanoparticle (adapted from Ref. [157]).

9. Summary and Outlook

Nanotechnology has touched upon every single modality of the molecular imaging arena (Table 1). For optical imaging, QDs have been the main focus and in vivo imaging has been achieved using either peptides or antibodies as the targeting ligand. The most well-studied contrast agents for

ers) in combination with efficient surface capping has been shown to substantially reduce desorption of core ions and render QDs more biologically inert for future applications.[155] Recently, nanotoxicology has emerged as a new branch of toxicology for studying the undesirable effects of nanoparticles.[165,166] Development of novel nanoplatforms for biomedical applications must proceed in tandem with the assessment of any toxicological side effects. Many currently accepted techniques faced much skepticism during their initial development. For example, radionuclide-based imaging was severely doubted a few decades ago and it is now routinely used in the clinic. It is just a matter of time before nanoplatform-based methods, upon further development and improvement, will be accepted by the public for routine clinical use.

The most promising applications of nanoplatform-based agents will be in cardiovascular medicine, where there are fewer biological barriers for the efficient delivery of nanoparticles, and in oncology, where the leaky tumor vasculature can allow for better tissue penetration than in normal organs/tissues. In many of the literature reports, it is not clear whether the nanoplatform-based imaging or therapeutic agents are actually targeting the vasculature or the (tumor) cells. It is likely that some nanoparticles do not extravasate at all or only extravasate to spaces in close proximity to the vessels, since most of the nanoparticles used so far are larger than 20 nm in diameter. Much care should be taken when interpreting the imaging data, target specificity, and targeting efficacy. Rigorous in vivo/ex vivo validation is needed before any nanoplatform-based agents enter the clinic.

Nanoplatform-based ex vivo protein nanosensors and in vivo imaging are both critical for future optimization of patient management. Ex vivo diagnostics in combination with in vivo diagnostics can provide a synergistic approach that neither strategy alone can offer. Upon further development and validation, nanoplatform-based approaches (both ex vivo nanosensing and in vivo imaging) will eventually be able to predict which patients will likely respond to a specific molecular therapy and monitor their response to personalized therapy. With the capacity to provide enormous sensitivity, throughput, and flexibility, nanoplatforms have the potential to profoundly impact disease diagnosis and patient management in the near future.

Acknowledgements

[1] M. Bruchez, Jr., M. Moronne, P. Gin, S. Weiss, A. P. Alivisatos, *Science* **1998**, *281*, 2013–2016.
[2] W. C. Chan, S. Nie, *Science* **1998**, *281*, 2016–2018.
[3] K. Balasubramanian, M. Burghard, *Small* **2005**, *1*, 180–192.
[4] L. Lacerda, A. Bianco, M. Prato, K. Kostarelos, *Adv. Drug Delivery Rev.* **2006**, *58*, 1460–1470.
[5] L. R. Hirsch, A. M. Gobin, A. R. Lowery, F. Tam, R. A. Drezek, N. J. Halas, J. L. West, *Ann. Biomed. Eng.* **2006**, *34*, 15–22.
[6] D. L. Thorek, A. K. Chen, J. Czupryna, A. Tsourkas, *Ann. Biomed. Eng.* **2006**, *34*, 23–38.
[7] M. Ferrari, *Nat. Rev. Cancer* **2005**, *5*, 161–171.
[8] P. Grodzinski, M. Silver, L. K. Molnar, *Expert Rev. Mol. Diagn.* **2006**, *6*, 307–318.
[9] M. A. Horton, A. Khan, *Nanomedicine* **2006**, *2*, 42–48.
[10] E. S. Kawasaki, A. Player, *Nanomedicine* **2005**, *1*, 101–109.
[11] A. M. Thayer, *Chem. Eng. News* **2007**, *85*, 15–21.
[12] S. K. Sahoo, S. Parveen, J. J. Panda, *Nanomedicine* **2007**, *3*, 20–31.
[13] R. Weissleder, U. Mahmood, *Radiology* **2001**, *219*, 316–333.
[14] T. F. Massoud, S. S. Gambhir, *Genes Dev.* **2003**, *17*, 545–580.
[15] W. Cai, J. Rao, S. S. Gambhir, X. Chen, *Mol. Cancer Ther.* **2006**, *5*, 2624–2633.
[16] T. Beyer, D. W. Townsend, T. Brun, P. E. Kinahan, M. Charron, R. Roddy, J. Jerin, J. Young, L. Byars, R. Nutt, *J. Nucl. Med.* **2000**, *41*, 1369–1379.
[17] E. Even-Sapir, H. Lerman, G. Lievshitz, A. Khafif, D. M. Fliss, A. Schwartz, E. Gur, Y. Skornick, S. Schneebaum, *J. Nucl. Med.* **2003**, *44*, 1413–1420.
[18] C. Catana, Y. Wu, M. S. Judenhofer, J. Qi, B. J. Pichler, S. R. Cherry, *J. Nucl. Med.* **2006**, *47*, 1968–1976.
[19] H. Maeda, J. Wu, T. Sawa, Y. Matsumura, K. Hori, *J. Controlled Release* **2000**, *65*, 271–284.
[20] T. Tanaka, S. Shiramoto, M. Miyashita, Y. Fujishima, Y. Kaneo, *Int. J. Pharm.* **2004**, *277*, 39–61.
[21] V. Ntziachristos, *Annu. Rev. Biomed. Eng.* **2006**, *8*, 1–33.
[22] R. M. Levenson, *Lab. Med.* **2004**, *35*, 244–251.
[23] J. R. Mansfield, K. W. Gossage, C. C. Hoyt, R. M. Levenson, *J. Biomed. Opt.* **2005**, *10*, 41207.
[24] V. Ntziachristos, C. H. Tung, C. Bremer, R. Weissleder, *Nat. Med.* **2002**, *8*, 757–760.
[25] X. Montet, V. Ntziachristos, J. Grimm, R. Weissleder, *Cancer Res.* **2005**, *65*, 6330–6336.
[26] P. Alivisatos, *Nat. Biotechnol.* **2004**, *22*, 47–52.
[27] X. Michalet, F. F. Pinaud, L. A. Bentolila, J. M. Tsay, S. Doose, J. J. Li, G. Sundaresan, A. M. Wu, S. S. Gambhir, S. Weiss, *Science* **2005**, *307*, 538–544.
[28] I. L. Medintz, H. T. Uyeda, E. R. Goldman, H. Mattoussi, *Nat. Mater.* **2005**, *4*, 435–446.
[29] A. P. Alivisatos, W. Gu, C. Larabell, *Annu. Rev. Biomed. Eng.* **2005**, *7*, 55–76.
[30] Z. B. Li, W. Cai, X. Chen, *J. Nanosci. Nanotechnol.* **2007**, *7*, 2567–2581.
[31] W. Cai, A. R. Hsu, Z. B. Li, X. Chen, *Nanoscale Res. Lett.* **2007**, *2*, 265–281.
[32] S. C. Pu, M. J. Yang, C. C. Hsu, C. W. Lai, C. C. Hsieh, S. H. Lin, Y. M. Cheng, P. T. Chou, *Small* **2006**, *2*, 1308–1313.
[33] D. R. Larson, W. R. Zipfel, R. M. Williams, S. W. Clark, M. P. Bruchez, F. W. Wise, W. W. Webb, *Science* **2003**, *300*, 1434–1436.
[34] C. Xu, W. Zipfel, J. B. Shear, R. M. Williams, W. W. Webb, *Proc. Natl. Acad. Sci. USA* **1996**, *93*, 10763–10768.
[35] Y. T. Lim, S. Kim, A. Nakayama, N. E. Stott, M. G. Bawendi, J. V. Frangioni, *Mol. Imaging* **2003**, *2*, 50–64.
[36] B. Dubertret, P. Skourides, D. J. Norris, V. Noireaux, A. H. Brivanlou, A. Libchaber, *Science* **2002**, *298*, 1759–1762.
[37] E. B. Voura, J. K. Jaiswal, H. Mattoussi, S. M. Simon, *Nat. Med.* **2004**, *10*, 993–998.

[38] S. Rieger, R. P. Kulkarni, D. Darcy, S. E. Fraser, R. W. Koster, *Dev. Dyn.* **2005**, *234*, 670–681.

[39] M. Stroh, J. P. Zimmer, D. G. Duda, T. S. Levchenko, K. S. Cohen, E. B. Brown, D. T. Scadden, V. P. Torchilin, M. G. Bawendi, D. Fukumura, R. K. Jain, *Nat. Med.* **2005**, *11*, 678–682.

[40] J. D. Smith, G. W. Fisher, A. S. Waggoner, P. G. Campbell, *Microvasc. Res.* **2007**, *73*, 75–83.

[41] S. Kim, Y. T. Lim, E. G. Soltesz, A. M. De Grand, J. Lee, A. Nakayama, J. A. Parker, T. Mihaljevic, R. G. Laurence, D. M. Dor, L. H. Cohn, M. G. Bawendi, J. V. Frangioni, *Nat. Biotechnol.* **2004**, *22*, 93–97.

[42] J. P. Zimmer, S. W. Kim, S. Ohnishi, E. Tanaka, J. V. Frangioni, M. G. Bawendi, *J. Am. Chem. Soc.* **2006**, *128*, 2526–2527.

[43] S. W. Kim, J. P. Zimmer, S. Ohnishi, J. B. Tracy, J. V. Frangioni, M. G. Bawendi, *J. Am. Chem. Soc.* **2005**, *127*, 10526–10532.

[44] B. Ballou, L. A. Ernst, S. Andreko, T. Harper, J. A. Fitzpatrick, A. S. Waggoner, M. P. Bruchez, *Bioconjugate Chem.* **2007**, *18*, 389–396.

[45] R. G. Thorne, C. Nicholson, *Proc. Natl. Acad. Sci. USA* **2006**, *103*, 5567–5572.

[46] H. Jackson, O. Muhammad, H. Daneshvar, J. Nelms, A. Popescu, M. A. Vogelbaum, M. Bruchez, S. A. Toms, *J. Neurosurg.* **2007**, *60*, 524–529; discussion 529–530.

[47] M. E. Akerman, W. C. W. Chan, P. Laakkonen, S. N. Bhatia, E. Ruoslahti, *Proc. Natl. Acad. Sci. USA* **2002**, *99*, 12617–12621.

[48] W. Cai, D. W. Shin, K. Chen, O. Gheysens, Q. Cao, S. X. Wang, S. S. Gambhir, X. Chen, *Nano Lett.* **2006**, *6*, 669–676.

[49] W. Cai, X. Chen, *Anti-Cancer Agents Med. Chem.* **2006**, *6*, 407–428.

[50] X. Chen, P. S. Conti, R. A. Moats, *Cancer Res.* **2004**, *64*, 8009–8014.

[51] W. Cai, Y. Wu, K. Chen, Q. Cao, D. A. Tice, X. Chen, *Cancer Res.* **2006**, *66*, 9673–9681.

[52] W. Cai, X. Zhang, Y. Wu, X. Chen, *J. Nucl. Med.* **2006**, *47*, 1172–1180.

[53] X. Gao, Y. Cui, R. M. Levenson, L. W. K. Chung, S. Nie, *Nat. Biotechnol.* **2004**, *22*, 969–976.

[54] X. Yu, L. Chen, K. Li, Y. Li, S. Xiao, X. Luo, J. Liu, L. Zhou, Y. Deng, D. Pang, Q. Wang, *J. Biomed. Opt.* **2007**, *12*, 014008.

[55] H. Tada, H. Higuchi, T. M. Wanatabe, N. Ohuchi, *Cancer Res.* **2007**, *67*, 1138–1144.

[56] N. Pradhan, D. M. Battaglia, Y. Liu, X. Peng, *Nano Lett.* **2007**, *7*, 312–317.

[57] N. Pradhan, X. Peng, *J. Am. Chem. Soc.* **2007**, *129*, 3339–3347.

[58] W. J. Mulder, R. Koole, R. J. Brandwijk, G. Storm, P. T. Chin, G. J. Strijkers, C. de Mello Donega, K. Nicolay, A. W. Griffioen, *Nano Lett.* **2006**, *6*, 1–6.

[59] S. T. Selvan, P. K. Patra, C. Y. Ang, J. Y. Ying, *Angew. Chem. Int. Ed.* **2007**, *46*, 2448–2452.

[60] A. F. Low, G. J. Tearney, B. E. Bouma, I. K. Jang, *Nat. Clin. Pract. Cardiovasc. Med.* **2006**, *3*, 154–162.

[61] A. G. Podoleanu, *Br. J. Radiol.* **2005**, *78*, 976–988.

[62] A. Agrawal, S. Huang, A. Wei Haw Lin, M. H. Lee, J. K. Barton, R. A. Drezek, T. J. Pfefer, *J. Biomed. Opt.* **2006**, *11*, 041121.

[63] C. Loo, A. Lin, L. Hirsch, M. H. Lee, J. Barton, N. Halas, J. West, R. Drezek, *Technol. Cancer Res. Treat.* **2004**, *3*, 33–40.

[64] H. Cang, T. Sun, Z. Y. Li, J. Chen, B. J. Wiley, Y. Xia, X. Li, *Opt. Lett.* **2005**, *30*, 3048–3050.

[65] M. Hu, J. Chen, Z. Y. Li, L. Au, G. V. Hartland, X. Li, M. Marquez, Y. Xia, *Chem. Prod. Chem. Soc. Rev.* **2006**, *35*, 1084–1094.

[66] J. Chen, I. R. Corbin, H. Li, W. Cao, J. D. Glickson, G. Zheng, *J. Am. Chem. Soc.* **2007**, *129*, 5798–5799.

[67] K. J. Mortele, J. McTavish, P. R. Ros, *Clin. Exp. Nephrol.* **2002**, *6*, 29–52.

[68] R. C. Nelson, J. L. Chezmar, J. E. Peterson, M. E. Bernardino, *AJR, Am. J. Roentgenol.* **1989**, *153*, 973–976.

[69] M. Remy-Jardin, J. Bahepar, J. J. Lafitte, P. Dequiedt, O. Ertzbischoff, J. Bruzzi, V. Delannoy-Deken, A. Duhamel, J. Remy, *Radiology* **2006**, *238*, 1022–1035.

[70] E. R. Wisner, A. Theon, S. M. Griffey, G. L. McIntire, *Invest. Radiol.* **2000**, *35*, 199–204.

[71] G. L. McIntire, E. R. Bacon, K. J. Illig, S. B. Coffey, B. Singh, G. Bessin, M. T. Shore, G. L. Wolf, *Invest. Radiol.* **2000**, *35*, 91–96.

[72] E. R. Wisner, R. W. Katzberg, D. P. Link, S. M. Griffey, C. M. Drake, A. R. Vessey, D. Johnson, P. J. Haley, *Acad. Radiol.* **1996**, *3*, 40–48.

[73] E. R. Wisner, R. W. Katzberg, S. M. Griffey, C. M. Drake, P. J. Haley, A. R. Vessey, *Acad. Radiol.* **1995**, *2*, 985–993.

[74] E. R. Wisner, R. W. Katzberg, P. D. Koblik, J. P. McGahan, S. M. Griffey, C. M. Drake, P. P. Harnish, A. R. Vessey, P. J. Haley, *Acad. Radiol.* **1995**, *2*, 405–412.

[75] E. R. Wisner, R. W. Katzberg, P. D. Koblik, D. K. Shelton, P. E. Fisher, S. M. Griffey, C. Drake, P. P. Harnish, A. R. Vessey, P. J. Haley, *Acad. Radiol.* **1994**, *1*, 377–384.

[76] F. Hyafil, J. C. Cornily, J. E. Feig, R. Gordon, E. Vucic, V. Amirbekian, E. A. Fisher, V. Fuster, L. J. Feldman, Z. A. Fayad, *Nat. Med.* **2007**, *13*, 636–641.

[77] O. Rabin, J. Manuel Perez, J. Grimm, G. Wojtkiewicz, R. Weissleder, *Nat. Mater.* **2006**, *5*, 118–122.

[78] S. H. Bloch, P. A. Dayton, K. W. Ferrara, *IEEE Eng. Med. Biol. Mag.* **2004**, *23*, 18–29.

[79] M. H. Wink, H. Wijkstra, J. J. De La Rosette, C. A. Grimbergen, *Minim. Invasive Ther. Allied Technol.* **2006**, *15*, 93–100.

[80] D. Cosgrove, *Eur. J. Radiol.* **2006**, *60*, 324–330.

[81] J. A. Jakobsen, *Eur. J. Dermatol. Eur. Radiol.* **2001**, *11*, 1329–1337.

[82] E. Stride, N. Saffari, *Proc. Inst. Mech. Eng., Part H* **2003**, *217*, 429–447.

[83] B. A. Kaufmann, J. R. Lindner, *Curr. Opin. Biotechnol.* **2007**, *18*, 11–16.

[84] D. B. Ellegala, H. Leong-Poi, J. E. Carpenter, A. L. Klibanov, S. Kaul, M. E. Shaffrey, J. Sklenar, J. R. Lindner, *Circulation* **2003**, *108*, 336–341.

[85] H. Leong-Poi, J. Christiansen, A. L. Klibanov, S. Kaul, J. R. Lindner, *Circulation* **2003**, *107*, 455–460.

[86] H. Leong-Poi, J. Christiansen, P. Heppner, C. W. Lewis, A. L. Klibanov, S. Kaul, J. R. Lindner, *Circulation* **2005**, *111*, 3248–3254.

[87] G. Korpanty, J. G. Carbon, P. A. Grayburn, J. B. Fleming, R. A. Brekken, *Clin. Cancer Res.* **2007**, *13*, 323–330.

[88] J. K. Willmann, R. Paulmurugan, K. Chen, O. Gheysens, M. Rodriguez-Porcel, A. M. Lutz, I. Y. Chen, X. Chen, S. S. Gambhir, *Radiology*, in press.

[89] G. M. Lanza, D. R. Abendschein, C. S. Hall, M. J. Scott, D. E. Scherrer, A. Houseman, J. G. Miller, S. A. Wickline, *J. Am. Soc., Echocardiogr.* **2000**, *13*, 608–614.

[90] G. M. Lanza, D. R. Abendschein, C. S. Hall, J. N. Marsh, M. J. Scott, D. E. Scherrer, S. A. Wickline, *Invest. Radiol.* **2000**, *35*, 227–234.

[91] M. S. Hughes, J. N. Marsh, H. Zhang, A. K. Woodson, J. S. Allen, E. K. Lacy, C. Carradine, G. M. Lanza, S. A. Wickline, *IEEE Trans. Ultrason. Ferroelectr. Freq. Control* **2006**, *53*, 1609–1616.

[92] A. P. Pathak, B. Gimi, K. Glunde, E. Ackerstaff, D. Artemov, Z. M. Bhujwalla, *Methods Enzymol.* **2004**, *386*, 3–60.

[93] Z. Zhang, S. A. Nair, T. J. McMurry, *Curr. Med. Chem.* **2005**, *12*, 751–778.

[94] R. G. Pautler, S. E. Fraser, *Curr. Opin. Immunol.* **2003**, *15*, 385–392.

[95] A. de Roos, J. Doornbos, D. Baleriaux, H. L. Bloem, T. H. Falke in *Magnetic Resonance Annual 1988* (Ed.: H. Y. Kressel), Raven Press, NY, **1988**, pp. 113–145.

[96] M. D. Chavanpatil, A. Khdair, J. Panyam, *J. Nanosci. Nanotechnol.* **2006**, *6*, 2651–2663.

[97] K. Shamsi, T. Balzer, S. Saini, P. R. Ros, R. C. Nelson, E. C. Carter, S. Tollerfield, H. P. Niendorf, *Radiology* **1998**, *206*, 365–371.

[98] P. Reimer, N. Jahnke, M. Fiebich, W. Schima, F. Deckers, C. Marx, N. Holzknecht, S. Saini, *Radiology* **2000**, *217*, 152–158.

[99] R. Weissleder, P. F. Hahn, D. D. Stark, G. Elizondo, S. Saini, L. E. Todd, J. Wittenberg, J. T. Ferrucci, *Radiology* **1988**, *169*, 399–403.

[100] R. Weissleder, D. D. Stark, E. J. Rummeny, C. C. Compton, J. T. Ferrucci, *Radiology* **1988**, *166*, 423–430.

[101] M. G. Mack, J. O. Balzer, R. Straub, K. Eichler, T. J. Vogl, *Radiology* **2002**, *222*, 239–244.

[102] Y. Anzai, C. W. Piccoli, E. K. Outwater, W. Stanford, D. A. Bluemke, P. Nurenberg, S. Saini, K. R. Maravilla, D. E. Feldman, U. P. Schmiedl, J. A. Brunberg, I. R. Francis, S. E. Harms, P. M. Som, C. M. Tempany, *Radiology* **2003**, *228*, 777–788.

[103] C. Zimmer, R. Weissleder, K. Poss, A. Bogdanova, S. C. Wright, Jr., W. S. Enochs, *Radiology* **1995**, *197*, 533–538.

[104] A. Moore, E. Marecos, A. Bogdanov, Jr., R. Weissleder, *Radiology* **2000**, *214*, 568–574.

[105] M. G. Harisinghani, J. Barentsz, P. F. Hahn, W. M. Deserno, S. Tabatabaei, C. H. van de Kaa, J. de La Rosette, R. Weissleder, *N. Engl. J. Med.* **2003**, *348*, 2491–2499.

[106] A. Saleh, M. Schroeter, C. Jonkmanns, H. P. Hartung, U. Modder, S. Jander, *Brain* **2004**, *127*, 1670–1677.

[107] V. Dousset, B. Brochet, M. S. Deloire, L. Lagoarde, B. Barroso, J. M. Caille, K. G. Petry, *Am. J. Neuroradiol.* **2006**, *27*, 1000–1005.

[108] W. S. Enochs, G. Harsh, F. Hochberg, R. Weissleder, *J. Magn. Reson. Imaging* **1999**, *9*, 228–232.

[109] C. Corot, K. G. Petry, R. Trivedi, A. Saleh, C. Jonkmanns, J. F. Le Bas, E. Blezer, M. Rausch, B. Brochet, P. Foster-Gareau, D. Baleriaux, S. Gaillard, V. Dousset, *Invest. Radiol.* **2004**, *39*, 619–625.

[110] E. M. Shapiro, S. Skrtic, K. Sharer, J. M. Hill, C. E. Dunbar, A. P. Koretsky, *Proc. Natl. Acad. Sci. USA* **2004**, *101*, 10901–10906.

[111] E. M. Shapiro, K. Sharer, S. Skrtic, A. P. Koretsky, *Magn. Reson. Med.* **2006**, *55*, 242–249.

[112] C. Heyn, J. A. Ronald, L. T. Mackenzie, I. C. MacDonald, A. F. Chambers, B. K. Rutt, P. J. Foster, *Magn. Reson. Med.* **2006**, *55*, 23–29.

[113] D. J. Stuckey, C. A. Carr, E. Martin-Rendon, D. J. Tyler, C. Willmott, P. J. Cassidy, S. J. Hale, J. E. Schneider, L. Tatton, S. E. Harding, G. K. Radda, S. Watt, K. Clarke, *Stem Cells* **2006**, *24*, 1968–1975.

[114] A. S. Arbab, E. K. Jordan, L. B. Wilson, G. T. Yocum, B. K. Lewis, J. A. Frank, *Hum. Gene Ther.* **2004**, *15*, 351–360.

[115] J. M. Hill, A. J. Dick, V. K. Raman, R. B. Thompson, Z. X. Yu, K. A. Hinds, B. S. Pessanha, M. A. Guttman, T. R. Varney, B. J. Martin, C. E. Dunbar, E. R. McVeigh, R. J. Lederman, *Circulation* **2003**, *108*, 1009–1014.

[116] I. J. de Vries, W. J. Lesterhuis, J. O. Barentsz, P. Verdijk, J. H. van Krieken, O. C. Boerman, W. J. Oyen, J. J. Bonenkamp, J. B. Boezeman, G. J. Adema, J. W. Bulte, T. W. Scheenen, C. J. Punt, A. Heerschap, C. G. Figdor, *Nat. Biotechnol.* **2005**, *23*, 1407–1413.

[117] E. T. Ahrens, M. Feili-Hariri, H. Xu, G. Genove, P. A. Morel, *Magn. Reson. Med.* **2003**, *49*, 1006–1013.

[118] W. S. Seo, J. H. Lee, X. Sun, Y. Suzuki, D. Mann, Z. Liu, M. Terashima, P. C. Yang, M. V. McConnell, D. G. Nishimura, H. Dai, *Nat. Mater.* **2006**, *5*, 971–976.

[119] W. Cai, S. S. Gambhir, X. Chen, *Biotechniques* **2005**, *39*, S6–S17.

[120] D. E. Sosnovik, R. Weissleder, *Curr. Opin. Biotechnol.* **2007**, *18*, 4–10.

[121] D. A. Sipkins, D. A. Cheresh, M. R. Kazemi, L. M. Nevin, M. D. Bednarski, K. C. Li, *Nat. Med.* **1998**, *4*, 623–626.

[122] S. A. Anderson, R. K. Rader, W. F. Westlin, C. Null, D. Jackson, G. M. Lanza, S. A. Wickline, J. J. Kotyk, *Magn. Reson. Med.* **2000**, *44*, 433–439.

[123] P. M. Winter, S. D. Caruthers, A. Kassner, T. D. Harris, L. K. Chinen, J. S. Allen, E. K. Lacy, H. Zhang, J. D. Robertson, S. A. Wickline, G. M. Lanza, *Cancer Res.* **2003**, *63*, 5838–5843.

[124] P. M. Winter, A. M. Morawski, S. D. Caruthers, R. W. Fuhrhop, H. Zhang, T. A. Williams, J. S. Allen, E. K. Lacy, J. D. Robertson, G. M. Lanza, S. A. Wickline, *Circulation* **2003**, *108*, 2270–2274.

[125] A. H. Schmieder, P. M. Winter, S. D. Caruthers, T. D. Harris, T. A. Williams, J. S. Allen, E. K. Lacy, H. Zhang, M. J. Scott, G. Hu, J. D. Robertson, S. A. Wickline, G. M. Lanza, *Magn. Reson. Med.* **2005**, *53*, 621–627.

[126] P. M. Winter, A. M. Neubauer, S. D. Caruthers, T. D. Harris, J. D. Robertson, T. A. Williams, A. H. Schmieder, G. Hu, J. S. Allen, E. K. Lacy, H. Zhang, S. A. Wickline, G. M. Lanza, *Arterioscler. Thromb. Vasc. Biol.* **2006**, *26*, 2103–2109.

[127] S. Flacke, S. Fischer, M. J. Scott, R. J. Fuhrhop, J. S. Allen, M. McLean, P. Winter, G. A. Sicard, P. J. Gaffney, S. A. Wickline, G. M. Lanza, *Circulation* **2001**, *104*, 1280–1285.

[128] G. M. Lanza, X. Yu, P. M. Winter, D. R. Abendschein, K. K. Karukstis, M. J. Scott, L. K. Chinen, R. W. Fuhrhop, D. E. Scherrer, S. A. Wickline, *Circulation* **2002**, *106*, 2842–2847.

[129] I. Paschkunova-Martic, C. Kremser, K. Mistlberger, N. Shcherbakova, H. Dietrich, H. Talasz, Y. Zou, B. Hugl, M. Galanski, E. Solder, K. Pfaller, I. Holiner, W. Buchberger, B. Keppler, P. Debbage, *Histochem. Cell Biol.* **2005**, *123*, 283–301.

[130] J. C. Frias, Y. Ma, K. J. Williams, Z. A. Fayad, E. A. Fisher, *Nano Lett.* **2006**, *6*, 2220–2224.

[131] Y. E. Koo, W. Fan, H. Hah, H. Xu, D. Orringer, B. Ross, A. Rehemtulla, M. A. Philbert, R. Kopelman, *Appl. Opt.* **2007**, *46*, 1924–1930.

[132] Y. W. Jun, Y. M. Huh, J. S. Choi, J. H. Lee, H. T. Song, S. Kim, S. Yoon, K. S. Kim, J. S. Shin, J. S. Suh, J. Cheon, *J. Am. Chem. Soc.* **2005**, *127*, 5732–5733.

[133] J. H. Lee, Y. M. Huh, Y. W. Jun, J. W. Seo, J. T. Jang, H. T. Song, S. Kim, E. J. Cho, H. G. Yoon, J. S. Suh, J. Cheon, *Nat. Med.* **2007**, *13*, 95–99.

[134] K. Peremans, B. Cornelissen, B. Van Den Bossche, K. Audenaert, C. Van de Wiele, *Vet. Radiol. Ultrasound* **2005**, *46*, 162–170.

[135] A. Kjaer, *Adv. Exp. Med. Biol.* **2006**, *587*, 277–284.

[136] S. J. DeNardo, G. L. DeNardo, L. A. Miers, A. Natarajan, A. R. Foreman, C. Gruettner, G. N. Adamson, R. Ivkov, *Clin. Cancer Res.* **2005**, *11*, 7087–7092.

[137] S. J. DeNardo, G. L. DeNardo, A. Natarajan, L. A. Miers, A. R. Foreman, C. Gruettner, G. N. Adamson, R. Ivkov, *J. Nucl. Med.* **2007**, *48*, 437–444.

[138] G. Hu, M. Lijowski, H. Zhang, K. C. Partlow, S. D. Caruthers, G. Kiefer, G. Gulyas, P. Athey, M. J. Scott, S. A. Wickline, G. M. Lanza, *Int. J. Cancer* **2007**, *120*, 1951–1957.

[139] D. S. Berman, H. Kiat, K. Van Train, J. D. Friedman, F. P. Wang, G. Germano, *Cardiovasc. Clin.* **1994**, *12*, 261–270.

[140] M. E. Phelps, E. J. Hoffman, N. A. Mullani, M. M. Ter-Pogossian, *J. Nucl. Med.* **1975**, *16*, 210–224.

[141] M. E. Phelps, *J. Nucl. Med.* **2000**, *41*, 661–681.

[142] S. R. Cherry, Y. Shao, R. W. Silverman, K. Meadors, S. Siegel, A. Chatziioannou, J. W. Young, W. F. Jones, J. C. Moyers, D. Newport, A. Boutefnouchet, T. H. Farquhar, M. Andreaco, M. J. Paulus, D. M. Binkley, R. Nutt, M. E. Phelps, *IEEE Trans. Nucl. Sci.* **1997**, *44*, 1161–1166.

[143] A. F. Chatziioannou, S. R. Cherry, Y. Shao, R. W. Silverman, K. Meadors, T. H. Farquhar, M. Pedarsani, M. E. Phelps, *J. Nucl. Med.* **1999**, *40*, 1164–1175.

[144] Z. Liu, W. Cai, L. He, N. Nakayama, K. Chen, X. Sun, X. Chen, H. Dai, *Nat. Nanotechnol.* **2007**, *2*, 47–52.

[145] W. J. Mulder, G. J. Strijkers, J. W. Habets, E. J. Bleeker, D. W. van der Schaft, G. Storm, G. A. Koning, A. W. Griffioen, K. Nicolay, *FASEB J.* **2005**, *19*, 2008–2010.

[146] M. F. Kircher, R. Weissleder, L. Josephson, *Bioconjugate Chem.* **2004**, *15*, 242–248.

[147] A. Tsourkas, V. R. Shinde-Patil, K. A. Kelly, P. Patel, A. Wolley, J. R. Allport, R. Weissleder, *Bioconjugate Chem.* **2005**, *16*, 576–581.

[148] M. Funovics, X. Montet, F. Reynolds, R. Weissleder, L. Josephson, *Neoplasia* **2005**, *7*, 904–911.

[149] K. A. Kelly, J. R. Allport, A. Tsourkas, V. R. Shinde-Patil, L. Josephson, R. Weissleder, *Circ. Res.* **2005**, *96*, 327–336.

[150] M. Nahrendorf, F. A. Jaffer, K. A. Kelly, D. E. Sosnovik, E. Aikawa, P. Libby, R. Weissleder, *Circulation* **2006**, *114*, 1504–1511.

[151] X. Montet, R. Weissleder, L. Josephson, *Bioconjugate Chem.* **2006**, *17*, 905–911.

[152] D. E. Sosnovik, E. A. Schellenberger, M. Nahrendorf, M. S. Novikov, T. Matsui, G. Dai, F. Reynolds, L. Grazette, A. Rosenzweig, R. Weissleder, L. Josephson, *Magn. Reson. Med.* **2005**, *54*, 718–724.

[153] W. Cai, K. Chen, Z. B. Li, S. S. Gambhir, X. Chen, *J. Nucl. Med.* **2007**, in press.

[154] C. Kirchner, T. Liedl, S. Kudera, T. Pellegrino, A. M. Javier, H. E. Gaub, S. Stoelzle, N. Fertig, W. J. Parak, *Nano Lett.* **2005**, *5*, 331–338.

[155] A. M. Derfus, W. C. W. Chan, S. N. Bhatia, *Nano Lett.* **2004**, *4*, 11–18.

[156] S. W. Zielhuis, J. H. Seppenwoolde, V. A. Mateus, C. J. Bakker, G. C. Krijger, G. Storm, B. A. Zonnenberg, A. D. van het Schip, G. A. Koning, J. F. Nijsen, *Cancer Biother. Radiopharm.* **2006**, *21*, 520–527.

[157] Z. Medarova, W. Pham, C. Farrar, V. Petkova, A. Moore, *Nat. Med.* **2007**, *13*, 372–377.

[158] A. Fire, S. Xu, M. K. Montgomery, S. A. Kostas, S. E. Driver, C. C. Mello, *Nature* **1998**, *391*, 806–811.

[159] M. Stevenson, *N. Engl. J. Med.* **2004**, *351*, 1772–1777.

[160] C. C. Mello, D. Conte, Jr., *Nature* **2004**, *431*, 338–342.

[161] M. Mae, U. Langel, *Curr. Opin. Pharmacol.* **2006**, *6*, 509–514.

[162] S. El-Andaloussi, T. Holm, U. Langel, *Curr. Pharm. Des.* **2005**, *11*, 3597–3611.

[163] A. C. Samia, X. Chen, C. Burda, *J. Am. Chem. Soc.* **2003**, *125*, 15736–15737.

[164] R. Bakalova, H. Ohba, Z. Zhelev, M. Ishikawa, Y. Baba, *Nat. Biotechnol.* **2004**, *22*, 1360–1361.

[165] G. Oberdorster, E. Oberdorster, J. Oberdorster, *Environ. Health Perspect.* **2005**, *113*, 823–839.

[166] V. E. Kagan, H. Bayir, A. A. Shvedova, *Nanomedicine* **2005**, *1*, 313–316.